Electronic Supplementary Information

A new $[Co_{21}(H_2O)_4(OH)_{12}]^{30+}$ unit incorporated polyoxotungstate for sensitive detection of dichlorvos

Dongying Shi,* Chao-Jie Cui, Chun-Xiao Sun, Jun-Ping Du and Chun-Sen Liu*

Henan Provincial Key Laboratory of Surface & Interface Science, Zhengzhou University of Light Industry, Zhengzhou 450002, P. R. China

Authors for correspondence: shidongying@zzuli.edu.cn; chunsenliu@zzuli.edu.cn

Contents

Section S1 X-ray crystallography

Section S2 Characterization of $Co_{25}Si_6W_{60}$

Section S3 Electrochemical measurements

Section S4 Comparisons between this work and other works

Section S5 References

Section S1 X-ray crystallography

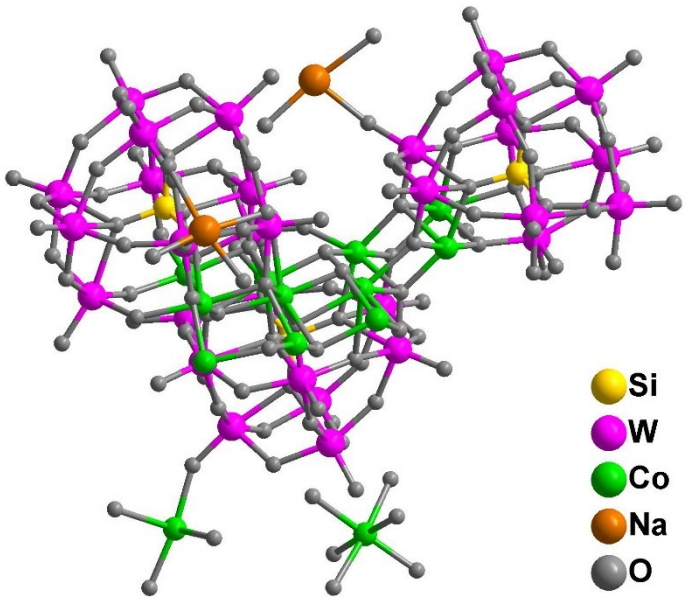

Fig. S1 Ball-and-stick representation of $Co_{25}Si_6W_{60}$ in an asymmetric unit.

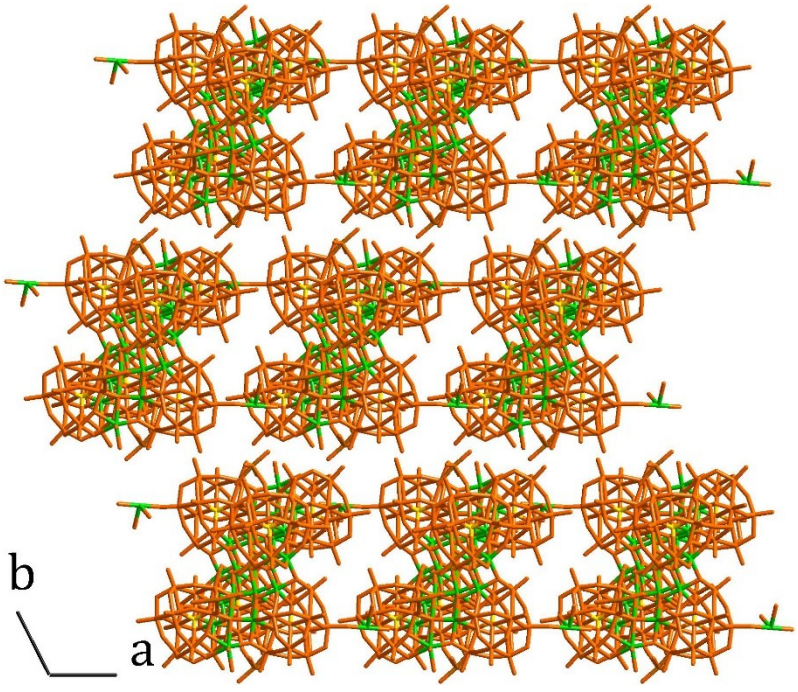

Fig. S2 View of the packing arrangement of $Co_{25}Si_6W_{60}$ along the *c* direction.

Table S1 Crystallographic data and structure refinement for **$Co_{25}Si_6W_{60}$**.

	$Co_{25}Si_6W_{60}$
Empirical formula	$Na_{22}O_{292}H_{128}Co_{25}Si_6W_{60}$
M, g·mol^{-1}	17978.85
Crystal system	Triclinic
Space group	P-1
a, Å	19.9421(6)
b, Å	23.2514(8)
c, Å	24.8961(8)
α, deg	98.678(3)
β, deg	110.845(3)
γ, deg	111.285(3)
V, Å^3	9518.3(5)
Z	1
D_{calcd}, g·cm^{-3}	3.052
T, K	293(2)
Refl. collected/unique	67770/37178 (R_{int} = 0.0746)
μ, mm^{-1}	41.753
GOF	1.019
R_1[a] / wR_2[b] ($I > 2\sigma(I)$)	0.0910 / 0.2525
R_1[a], wR_2[b] (all data)	0.1491 / 0.3022
Diff peak and hole, e·Å^{-3}	4.946 / –3.169

[a] $R_1 = \sum||F_o| - |F_c||/\sum|F_o|$. [b] $wR_2 = [\sum w(F_o^2 - F_c^2)^2/\sum w(F_o^2)^2]^{1/2}$; $w = 1/[\sigma^2(F_o^2) + (0.1727P)^2 + 0.0000P]$; $P = (F_o^2 + 2F_c^2)/3$.

Section S2 Characterization of $Co_{25}Si_6W_{60}$

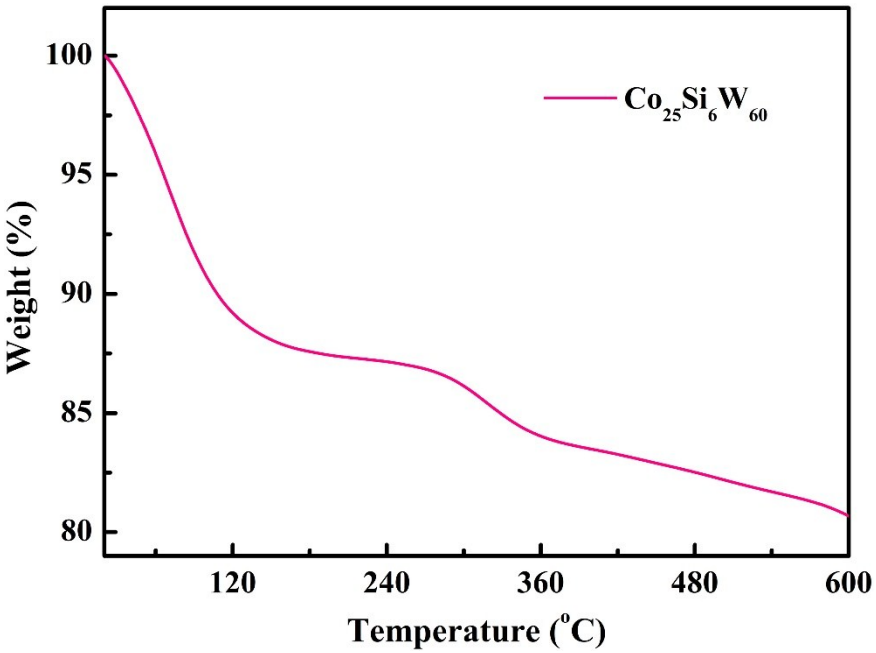

Fig. S3 The TGA curve of **$Co_{25}Si_6W_{60}$** under flowing N_2 atmosphere.

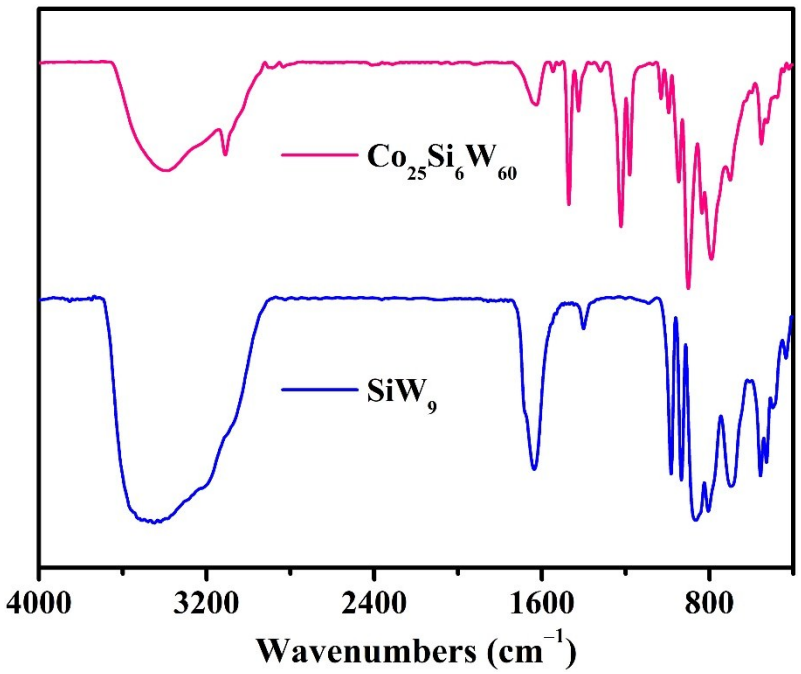

Fig. S4 The IR spectra of **$Co_{25}Si_6W_{60}$** and SiW_9.

Section S3 Electrochemical measurements

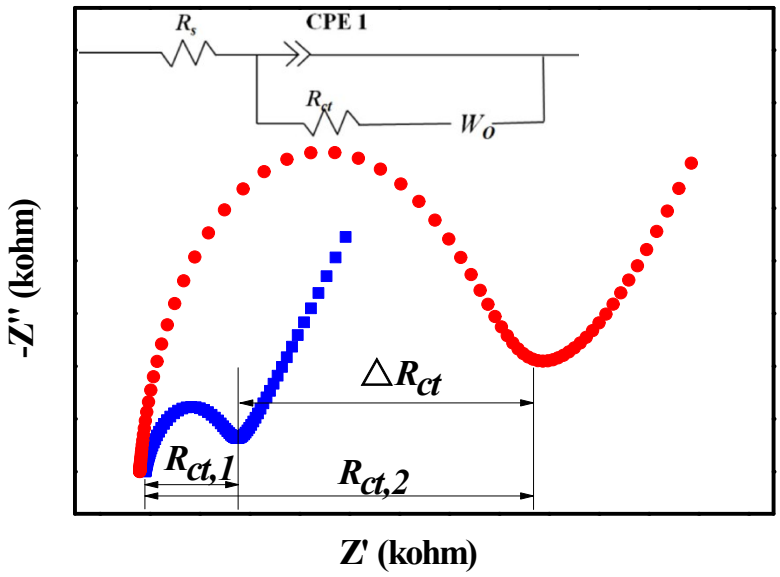

Fig. S5 EIS Nyquist plots and equivalent circuit.

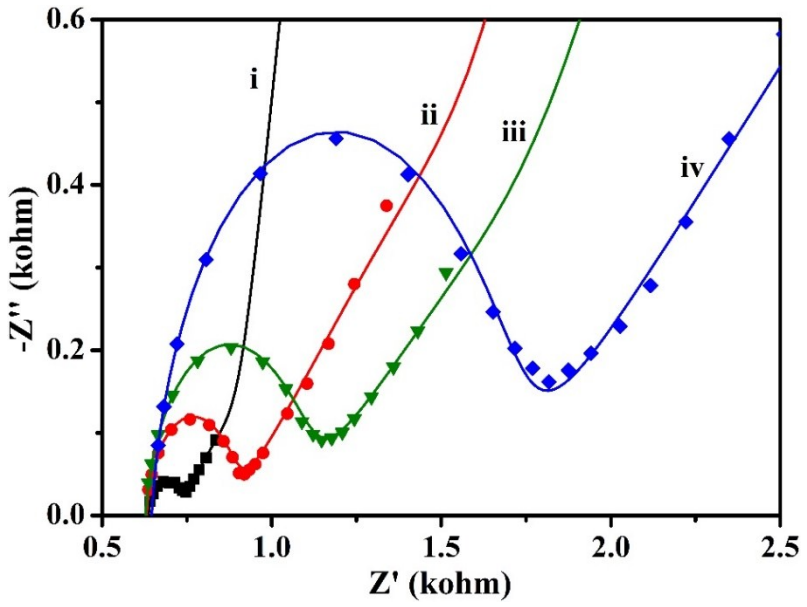

Fig. S6 EIS Nyquist plots for detecting DDV using the developed electrochemical biosensor based on $\mathbf{Co_{25}Si_6W_{60}}$ POM in 5 mM $[Fe(CN)_6]^{3-/4-}$ (0.1 M PBS, pH 7.4) containing 0.14 M NaCl and 1 M KCl: (i) bare AE, (ii) $\mathbf{Co_{25}Si_6W_{60}}$/AE, (iii) AChE/$\mathbf{Co_{25}Si_6W_{60}}$/AE, and (iv) DDV/AChE/$\mathbf{Co_{25}Si_6W_{60}}$/AE.

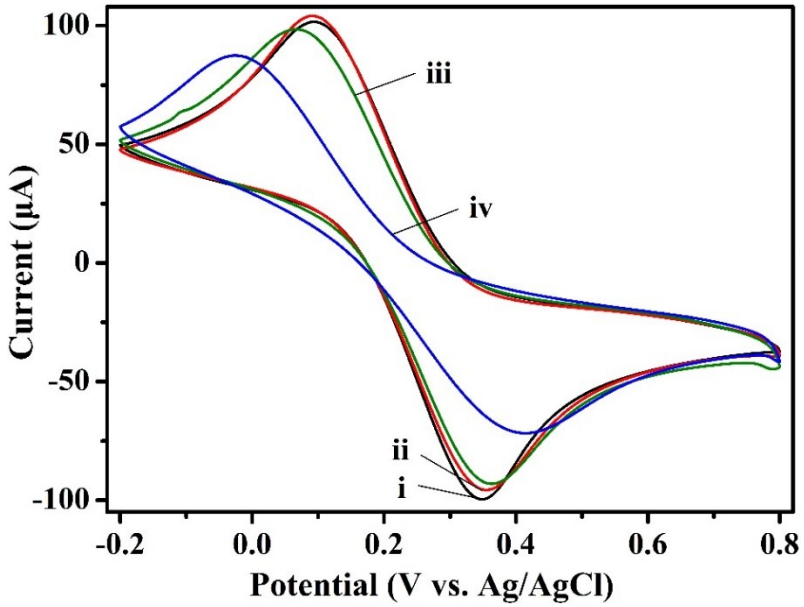

Fig. S7 CV curves for detecting DDV using the developed electrochemical biosensor based on $\mathbf{Co_{25}Si_6W_{60}}$ POM in 5 mM $[Fe(CN)_6]^{3-/4-}$ (0.1 M PBS, pH 7.4) containing 0.14 M NaCl and 1 M KCl: (i) bare AE, (ii) $\mathbf{Co_{25}Si_6W_{60}}$/AE, (iii) AChE/$\mathbf{Co_{25}Si_6W_{60}}$/AE, and (iv) DDV/AChE/$\mathbf{Co_{25}Si_6W_{60}}$/AE.

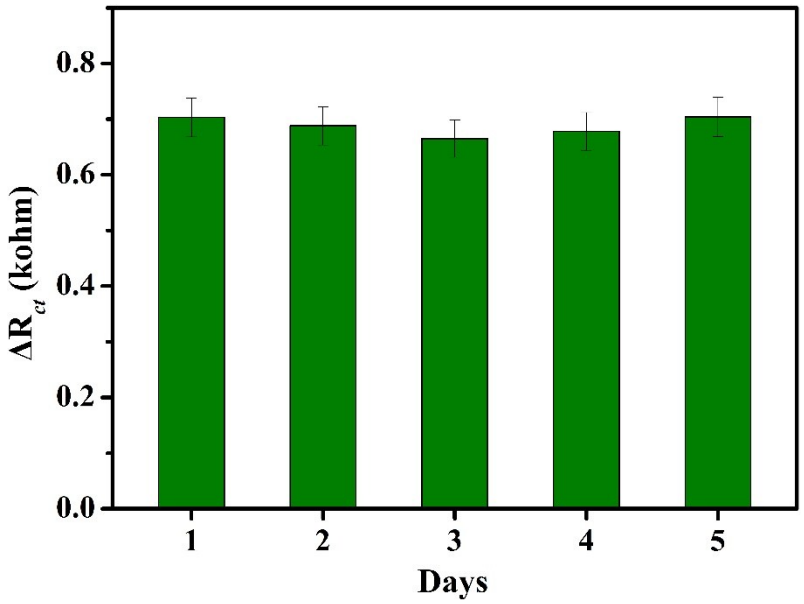

Fig. S8 Stability of the $\mathbf{Co_{25}Si_6W_{60}}$-based electrochemical biosensor for detecting DDV (0.001 $ng \cdot mL^{-1}$).

Table S2 Determination of DDV in Top-water by the $Co_{25}Si_6W_{60}$-based biosensor.

Added ($ng \cdot mL^{-1}$)	Found ($ng \cdot mL^{-1}$)	Apparent recovery (%)	RSD (%)
1.0	1.00	100.0	1.3
5.0	4.90	98.0	0.6
10.0	10.2	102.0	0.5
50.0	51.1	102.2	0.3
100.0	102.3	102.3	0.3

Section S4 Comparisons between this work and other works

Table S3 Comparisons of the proposed method with other DDV-detection methods.

Entry	Materials	Detection method	Line range	LOD
1	**$Co_{25}Si_6W_{60}$ (this work)**	**EIS**	**0.001–0.5 ng·mL^{-1}**	**0.30 pg·mL^{-1}**
2	Quenchbody[1]	Chromatographic analysis	0.1–50.0 μg·mL^{-1}	0.003 mg·kg^{-1}
3	Quenchbody[2]	Chromatographic analysis	0.06–2.4 μg·L^{-1}	0.016 μg·L^{-1}
4	QDs-nano-ZnTPyP[3]	Observe the change in fluorescence color	1–50 μg·L^{-1}	poor
5	Graphene quantum dots[4]	Luminescence	0.45–45.25 μM	0.778 μM
6	CS@TiO_2-CS/rGO[5]	EIS	0.036–22.6 μM	29 nM
7	Quenchbody[6]	Chromatographic analysis	58.8–225.5 ng·g^{-1}	7.3 ng·g^{-1}
8	Quenchbody[7]	Matrix solid-phase dispersion	0.2–2.6 μg·kg^{-1}	1.4 μg·kg^{-1}
9	Zinc oxide nanospheres[8]	cyclic voltammetry	Not reported	0.012 nM
10	[BSmim]HSO_4-AuNPs-porous carbon composite[9]	EIS	10^{-10}–10^{-6} g·L^{-1}	6.61 ×10^{-11} g·L^{-1}
11	Quenchbody[10]	Chromatographic analysis	0.05–30 ng·mL^{-1}	10 pg·mL^{-1}
12	Poly(4-aminophenol) modified graphite[11]	EIS	0.5–10 mmol·L^{-1}	0.8 μmol·L^{-1}
13	Al_2O_3 sol-gel[12]	Amperometric	0.1–80 μM	10 nM
14	Chromoionophore in sol-gel films[13]	Optical mode	0.5–7 mg·L^{-1}	0.5 mg·L^{-1}

Section S5 References

1 X. Qin, X. Luo, Y. Chen, J. Han, J. Zhang, K. Zhang and D. Hu, *Biomed. Chromatogr.*, 2019, **33**, 4537.

2 Q. T. Nguyen, C. Douny, M. P. Tran, F. Brose, P. T. Nguyen, D. T. T. Huong, P. Kestemont and M.-L. Scippo, *Aquac. Res.*, 2019, **50**, 247–255.

3 Q. Wang, Q. Yin, Y. Fan, L. Zhang, Y. Xu, O. Hu, X. Guo, Q. Shi, H. Fu and Y. She, *Talanta*, 2019, **199**, 46–53.

4 C. Sahub, T. Tuntulani, T. Nhujak and B. Tomapatanaget, *Sensor. Actuat. B-Chem.*, 2018, **258**, 88–97.

5 H.-F. Cui, W.-W. Wu, M.-M. Li, X. Song, Y. Lv and T.-T. Zhang, *Biosen. Bioelectron.*, 2018, **99**, 223–229.

6 A. Kumar, J. P. S. Gill, J. S. Bedi and A. Kumar, *Environ. Sci. Pollut. R.*, 2018, **25**, 34005–34016.

7 K. Medina-Dzul, S. Medina-Peralta, C. Carrera-Figueiras, M. Sánchez and D. Muñoz-Rodríguez, *Int. J. Environ. An. Ch.*, 2017, 1–10.

8 R. Sundarmurugasan, M. B. Gumpu, B. L. Ramachandra, N. Nesakumar, S. Sethuraman, U. M. Krishnan and J. B. B. Rayappan, *Sensor. Actuat. B-Chem.*, 2016, **230**, 306–313.

9 M. Wei and J. Wang, *Sensor. Actuat. B-Chem.*, 2015, **211**, 290–296.

10 L. Yin, X. Meng, X. Zhou, T. Zhang, H. Sun, Z. Yang, B. Yang, N. Xiao, J. P. Fawcett, Y. Yang and J. Gu, *J. Chromatogr. B*, 2015, **998–999**, 8–14.

11 E. I. Melo, D. L. Franco, A. S. Afonso, H. C. Rezende, A. G. Brito-Madurro, J. M. Madurro and N. M. M. Coelho, *Braz. Arch. Biol. Technol.*,2011, **54**, 1217–1222.

12 M. Shi, J. Xu, S. Zhang, B. Liu and J. Kong, *Talanta*, 2006, **68**, 1089–1095.

13 F. Wong, M. Ahmad, L. Y. Heng, L. B. Peng, *Talanta*, 2006, **69**, 888–893.